Chafer-Dolz, B.; Cecilia-Canales, JM.; Imbernón, B.; Nuñez-Delicado, E.; Casaña-Giner, V.; Cerón-Carrasco, JP. (2023). Insecticide discovery by drug repurposing: new synergistic inhibitors against Periplaneta americana. New Journal of Chemistry. 47(37):17234-17243. https://doi.org/10.1039/d3nj02676k

NJC

ARTICLE TYPE

Cite this: DOI: 00.0000/xxxxxxxxxx

Insecticide discovery by drug repurposing: new synergistic inhibitors against *Periplaneta americana*†

Beatriz Chafer-Dolz,*[a] José M. Cecilia,[b], Baldomero Imbernón,[c] Estrella Núñez-Delicado,[c] Victor Casaa-Giner[a] and José P. Cerón-Carrasco*[d]

Received Date
Accepted Date

DOI: 00.0000/xxxxxxxxxx

Virtual screening (VS) procedures have been widely used to accelerate the drug discovery process. They have also been implemented in other fields such as catalysts, energetic materials and more recently into the design of novel insecticides. The latter is an industrial priority to meet current legislation. Particularly challenging are cockroaches: they are associated to a number of diseases while the available solutions are harmful to humans. Herein, we performed an *in silico* and *in vivo* screening of the Drug Bank (DB) database for new potential voltage-dependent sodium channel (VGSC) synergists against American cockroach (*Periplaneta americana*). The VS pipeline procedure implements two ligand-based methods, e.g., Glide and METADOCK 2.0, which are further refined by rescoring. The most promising compounds are tested with *in vivo* models. Our combined computational and theoretical scheme leads to the discovery of miglitol as a new effective synergistic compound when combined with commercial formulations. Miglitol speeds up the overall knockout time by a factor of 12X while providing 100% of mortality after 24 hours. These results open the door to enhanced insecticides as well as to a wider use of VS methods.

1 Introduction

Cockroaches have been in close contact with humans since time immemorial.[1,2] More than four thousand cockroach species have been identified, of which 30 are harmful to humans.[3] In particular, the American cockroach (*Periplaneta americana*) physically transmits pathogens including viruses, bacteria, fungi and moulds, which cause diarrhoea, dysentery, cholera, leprosy, plague, typhoid fever and viral diseases such as polio.[4] The development of efficient biocides has been selected as a priority research line by the World Health Organisation (WHO).[5]

Voltage-activated sodium channels (Na_v) constitute a major target for controlling if not eradicate insects. Indeed, Na_v plays a critical role in generating membrane excitability[6] and are the target of numerous chemical insecticides, human drugs and poisonous neurotoxins. A recent work by Shen *et al.*[7] represents one of the main advances in that framework, as these authors reported the cryogenic electron microscopy structure of a putative Na_v channel from American cockroach (labelled hereafter as Na_vPaS) at 2.60 Åresolution. The available experimental data – that includes the position and interaction of inhibitors – is a cornerstone for performing computational models. That structural data motivated the present contribution that deals with the use of molecular and *in vivo* models in the search of enhanced insecticides against cockroaches.

Until now, most of the household insecticides are based on pyrethroids, a family of compound that disrupt the nervous system by targeting the voltage-dependent sodium channel (VGSC).[8,9] As a result, the membranes of electrically excitable

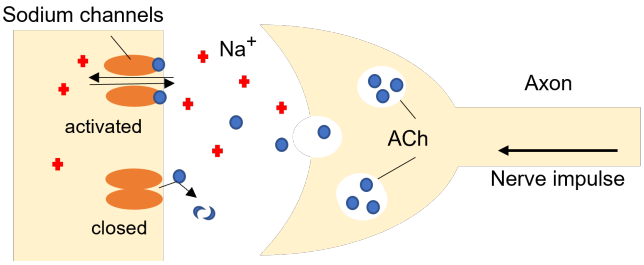

Fig. 1 Schematic representation of sodium channels and an intervening synapse.

[a] *Bio Logic Crop Science, S.L. Amadeo de Saboya 1-4, 46010, Valencia, Spain; E-mail: bchafer@biologiccropscience.com*
[b] *Universitat Politécnica de Valencia (UPV). Camino de Vera S/N, 46022, Valencia, Spain.*
[c] *Universidad Católica San Antonio de Murcia (UCAM). Campus de los Jerónimos, 30107, Murcia, Spain.*
[d] *Centro Universitario de la Defensa, Academia General del Aire. Universidad Politécnica de Cartagena. C/ Coronel López Peña s/n 30729. Santiago de la Ribera, Murcia, Spain; E-mail: jose.ceron@cud.upct.es*

† Electronic Supplementary Information (ESI) available: (a) metaheuristic parameters used for *METADOCK*2.0; (b) METADOCK 2.0 parameter settings obtained from the HYPERDOCK software; (c) main ingredients, solvents and emulsifiers used for *in vivo* testing, including CAS number and commercial supplier; (d) PDB structures of top-ranked compounds predicted by both standard workflow and enhanced sampling. See DOI: 00.0000/00000000.

cells become persistently depolarized and the insect is rapidly paralysed and dies, often exhibiting a "knock-down" response. However, the long persistence of pyrethroids in soils[10] and, more recently in other animals such as fish,[11] has led in recent years to control/limit their use. In that framework, the discover of a synergist might help to circumvent current insecticide solutions by reducing the response time (measured as Knockdown time, KD) and/or increasing mortality.[12]

Virtual screening (VS) methods based on docking simulations are well-suited to find these new or alternative molecules. They have been traditionally used to enhance the drug discovery process by screening large databases of chemical compounds (i.e., ligands) to find new drug candidates that bind to a specific biological target.[13–15] There are several codes to carry out molecular docking[16]. For instance, AutoDock,[17] Glide,[18] BUDE,[19] or DOCK[20] are able to perform simulation on the protein surface. These methods are usually guided by the position of a particular ligand in the protein-ligand complex, with a focus on a specific binding region (i.e., binding site) while other regions of the protein that might have activity remain unexplored. Alternative molecular docking tools such as BINDSURF[21] or METADOCK[22,23] perform the so-called "blind-docking" regimen, e.g., an unbiased search on the whole protein surface by dividing into arbitrary independent regions (or spots). Such blind-docking scheme is certainly more demanding than standard docking methods as simulations are performed simultaneously at all available pockets on the protein rather than being restricted to the binding site area. In addition, the success of VS strongly depends on the ability of the method to correctly rank candidates according to the estimated affinity or scoring.[24,25] This is a critical step in the classical drug discovery pipeline as only the best ranked leads are continue the process roadmap that goes from *in vitro* studies to *in vivo* investigations and, eventually, to human trials.[13]

Inspired by all these accumulated findings, herein we propose a refined VS pipeline to find new chemical compounds that inhibit the American cockroach Na_vPaS. Our main goal is to expand the chemical space of search by repurposing old drugs as novel insecticides.

2 Computational and Experimental Methods

2.1 Chemical models: targeted structure and compound database

Na_v channels play a critical role in a wide range of living organism, including mammals, by regulating the in/out–transport of Na^+ cations in cells, a step required for the correct generation of the nerve impulse. It is therefore not surprising the huge clinical efforts devoted to modulate these channels in the treatment of nerve and muscle-related disorders.[26] A similar reasoning applies for insecticides but with an opposite goal: the use of toxins to block that membrane proteins in insects might disrupt their normal nerve impulses and in turn help to incapacitate a plague progression. Indeed, first insecticidal pyrethrins, modern synthetic pyrethroids as well as new pyrazoline-based derivatives all target sodium channels.[27]

Our starting material is the available Na_vPaS structure deposited in the protein data bank (PDB) with code 6A95. That structure was published by Shen and co-workers,[28] which is illustrated in Figure 2. As discussed by these authors, Na_vPaS inhibitors might be classified as pore blockers and gating modifiers. The former are associated to small molecules capable to block the core pore, while the latter interacts with the voltage-sensing domain.[7] The 6A95 structure has been resolved with a pore blocker, tetrodotoxin (TTX), which opens the door for performing computational models. The raw structural data of Na_vPaS was refined with default parameters implemented in the Protein Preparation Wizard Module by Schröringer.[29] That step complete the structure by including all missing hydrogen atoms, assigning bond orders[30] and defining charges with Epik at pH = 7.0.[31] The protonation states of all residues were computed with the PROPKA code.[32] A restricted optimization was finally carried out by minimizing all hydrogen atoms with the last OPLS4 force field.[33]

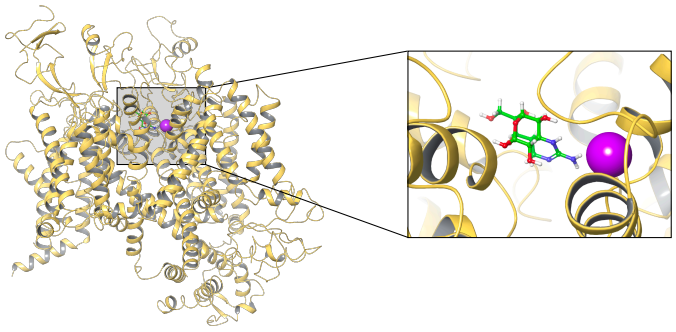

Fig. 2 Left panel: Experimental structure of the Na_vPaS in presence of the guanidinium pore blockers TTX. Protein is plotted as yellow cartoon. TTX inhibitor is displayed as ball and stick (colour scheme: carbon in green, oxygen, nitrogen in blue and hydrogen in White) and sodium atom located in the central pore (pink ball). Red panel: zoom into the binding site region.

As in any VS investigation, the source of compounds is a major parameter. Herein, we decided to go for a well-known library of compounds in the area of drug design, though less explored for developing insecticides. More specifically, our protocol based on screening the Drug Bank (DB) database,[34] which contains more than 10,000 compounds, including approved, nutraceutical, experimental and withdrawn drugs.[35] DB is consequent one of the prime sources of molecules in drug design so that it might be used to expand the chemical space of insecticides. DB contains molecules that target biomolecules present in human tissues, it might also results a promising source of candidates for discovering molecules compatible with targets present in other organisms as insects. The structures deposited in the DB database were downloaded and cured by using the LigPrep module implemented in Schrörindger, which assigns bond orders, determines protonation states at pH = 7.0 and optimizes structures with the same OPLS4 force field. That module is also used to generate all possible tautomers.[36] LigPrep was also used to model a set of pyrethroids that are used as positive controls: pyrethrin, piperonyl butoxide, cypermethrin, phenothrin and prallethrin.

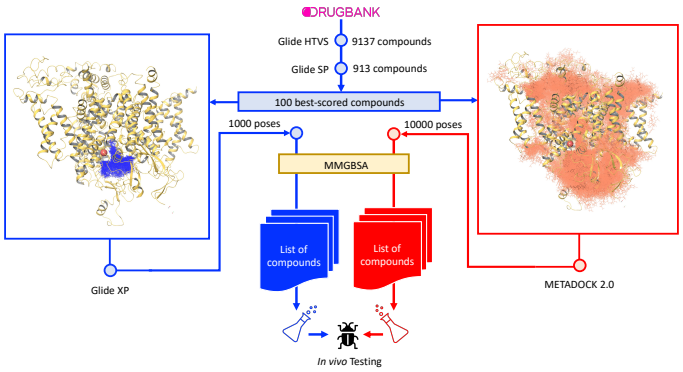

Fig. 3 Virtual screening strategies. The left panel illustrates the standard protocol implemented in Glide, which performs a three steps docking (HTVS, SP and XP) with a focus on the binding region of the small inhibitor (TTX). Best 100-ranked conformations are displayed in blue tubes and retained for MMGBSA refinement, which eventually lead to first list of compounds based on the standard protocol of Schrödinger. An alternative sampling is conducted by using these 100 compound as input for METADOCK 2.0, which search for best conformations along with all the Na_vPaS surface, displayed as red tubes. Outputs by METADOCK 2.0 are finally refined with MMGBSA to produce a second list of compounds. Both Glide and METADOCK hits are analyzed for *in vivo* testing.

2.2 VS pipeline

Figure 3 shows the VS strategy developed to target the Na_vPaS, which combines two main discovery schemes. As sketched, the former is based on the Glide workflow focused on the active site. A grid box of $20 \times 20 \times 20$ Å^3 is generated at the location of the crystallized TTX inhibitor. Once the grid is defined, all ligands went through the three stages of traditional GLIDE pipeline,[37,38] i.e., high throughput virtual screening (HTVS), standard precision (SP) and extra precision (XP) protocols. In that approach, the number of false positives are sequentially reduced from more than 10,000 hits to 1,000 at the HTVS step. It is worth stressing that both HTVS and SP implement the same scoring function. However, HTVS is based on a less demanding torsional refinement and sampling that allows to a quick rejection of compounds incompatible with the central pore. SP step is used to redock the best 1,000 hits generated by HTVS. The docking procedure is completed by redocking the 100 best-scored compounds with XP level of accuracy, which implements a more refined scoring function.[39] A maximum of 10 conformations are allowed in that final XP step.

Although that Glide three-level protocol allows for a fast screening of large libraries, the search is mainly restricted to an specific binding site. The number of generated conformations is also limited (i.e., up to 10 conformations per ligand). That approach keep computational cost under control as Glide exclusively uses CPU resources. METADOCK 2.0 is used to enhance the generation of conformations at such latter docking step. As discussed elsewhere,[23] METADOCK is a high throughput blind docking method based on a parallel parameterized metaheuristic scheme that runs on GPUs. This docking method is able to set up different search mechanisms based on metaheuristics procedures such as Genetic Algorithms (GAs), Greedy Search (GS), Scatter Search (SS), Hill Climbing, just to mention few. Search methods are defined by instantiating a set of configuration parameters that define the metaheuristic's stop condition, the number of individuals in the initial population, the combination policy, mutations, etc.† Accordingly, this parameter setting defines the effectiveness of the docking procedure, so several parameter optimizations must be performed before launching the simulation. This process is carried out by HYPERDOCK that develops a systematic search.[40,41]

The individuals of the metaheuristics are associated to conformations of the protein-ligand complex. For each ligand, a population of conformations is generated and distributed among the alpha-carbons on the protein surface. In this way, the entire surface of the receptor is systematically searched. To determine the goodness of a particular pose, the METADOCK 2.0 scoring function is calculated. We have previously assessed scoring functions from the literature,[23] including the scoring functions of AutoDock Vina,[42] Autodock 4.2[43] and BINDSURF.[21] Such earlier analysis revealed a trade-off between computation and prediction accuracy, which clearly benefited the AutoDock 4.0 scoring function. Our present implementation is consistent with that previous strategy. More specifically, the refinement phase developed by METADOCK 2.0 is fed by the 100 compounds with the highest affinity generated in the HTVS and SP stages. After the refinement phase, METADOCK 2.0 generates the 10 highest affinity conformations.

These docking methods generate a series of compounds that are sorted out according to its scoring value. We stress that the scoring functions of the methods are not equivalent, so the values obtained by Glide and METADOCK 2.0 are not directly comparable between them. It is important to note that though docking is a valuable tool for screening novel compounds against biotargets, such approaches might also lead to inactive molecules.[44] In that framework, post-refining should be implemented to further improve numeric outcomes. Aiming to both homogenize and refine the scoring values, the binding energies of the best-ranked Glide and METADOCK 2.0 hits are eventually recomputed with the MMGBSA method implemented in the Prime module.[45,46] MMGBSA allows to refine the obtained computational results, taking into account the energies before and after ligand binding, which in turn allows a more rigorous rescaling.[47–50] In this method, the ligand free energies are calculated as follows,

$$\Delta G_{bind} = G_{complex} - G_{target} - G_{ligand} \quad (1)$$

where ΔG_{bind} represents the binding-free energy of each ligand, and $G_{complex}$, G_{target}, and G_{ligand} are the free energies of complex, target (Na_vPaS), and ligand (DB entry), respectively. That equation might be rewritten as:

$$\Delta G_{bind}^{MMGBSA} = \Delta E_{MM} + \Delta G_{GB} + \Delta G_{SA} - T\Delta S \quad (2)$$

where ΔE_{MM} is the total energy in gas phase (including the internal, electrostatic and the van der Waals contributions), ΔG_{GB} is the polar contribution to the solvation free energy computed with generalized Born method, ΔG_{SA} is the nonpolar solvation free term predicted linear function of the solvent-accessible surface area (SASA), and $T\Delta S$ is the conformational entropy change.[51]

These terms yield to the binding-free energy of each ligand within the MMGBSA approach (ΔG_{bind}^{MMGBSA}).

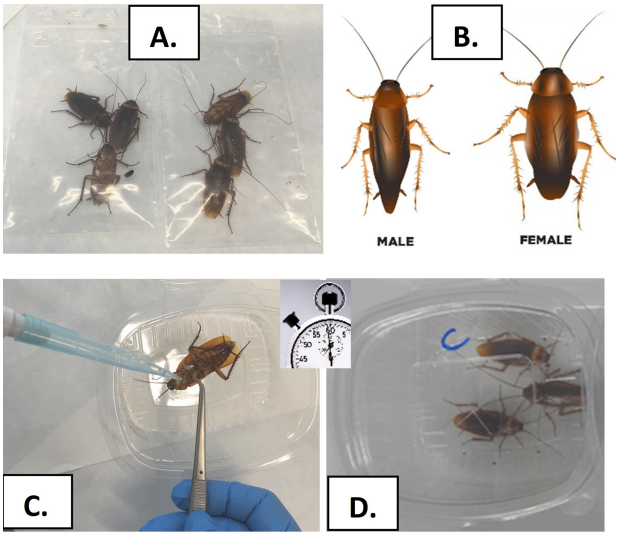

Fig. 4 Topical application methodology in American cockroach. A) Initial cockroaches sample, B) Morphology of male and female cockroaches, C) Topical application, D) Assessment phase.

2.3 *In vivo* models

The *in vivo* procedure to test the efficacy of the selected compounds on the American cockroach is restricted to available compounds on the market with tolerable toxicity and cost. As an additional prerequisite for real commercial formulations, compounds must be soluble in non-toxic solvents. The *in vivo* experiments have been carried out in the biological laboratories of the company Francisco Aragón S.L.U. (Murcia, Spain). They have been carried out on individual of *Periplaneta americana* from 3 different strains. The first and oldest strain was collected in 2008, at FA headquarter. 4 breeding lines of this insect were developed, thus providing all three stages of its life cycle: egg, nymph and adult. The second strain was purchased in 2018 from i2L Research Laboratory Ltd. (Cardiff, U.K.) and a new breeding line was created with this strain. The last strain under study was also collected in 2021 in Murcia (Spain), composed of nymphs and adults of American cockroaches, and a new breeding line was developed with this third strain. All cockroaches were reared at 27.5 ± 0.5 °C, 70 ± 5% Relative Humidity and a photoperiod of 12:12 (L:D) and they were fed with water and pet's food.

Figure 4 shows the methodology for *in vivo* testing to evaluate the synergistic activity. It is based on topical application methodology in which each substance to be tested is diluted to the suitable selected concentration in a 0.05% Prallethrin solution. The solvent depends on the solubility of each test substance to achieve the desired concentration (see Table 2). It should be stressed that the solvent itself guaranteed not to be toxic to the insect. Moreover, controls are established to identify the synergistic effect of the target compound. The control is based on the solvent used to dilute the target compound in a 0.05% prallethrin solution. The basic steps of our *in vivo* are conceived as follows:

1. Three females and three males of American cockroach are selected and placed in zip-closed bags.
2. To select the same number of males and females, we rely on fences/styles (morphology). Females have fences and no styles, and males have fences and styles.
3. The individual is immobilized with the help of tweezers and, with the micropipette of 10 μl, is dosed directly and individually, a drop of 5 μl. The area chosen for the application of the substances is in the ventral area.
4. Once the substance has been applied, the individual is placed in a plastic cup and the time it takes for the individual to flip over is observed; also known as the knockdown (KD) time.

To determine the synergistic activity of a substance on cockroaches, several *in vivo* metrics are recorded including KD time (KD50 means time to knock down 50% of the individuals), which quantifies the time course of action on the cockroach. This is of particular relevance in household insecticides, as users demand a quick response from the product, also favoring a reduction in the application of insecticides in the environment. We observe that cockroaches may flip over but recover after some time though, so the percentage of mortality after 60-minutes and 24-hours are also measured.

3 Results and discussion

3.1 Target validation

As described above, the target under study is Na_vPaS whose crystallographic structure is achieved with TTX. Therefore, Glide and METADOCK 2.0 should correctly reproduce the binding mode of the TTX ligand to the sodium channel. To summarize that early benchmark, the left-hand panel of Figure 5 overlays the experimental (red) structure with predicted conformation obtained by

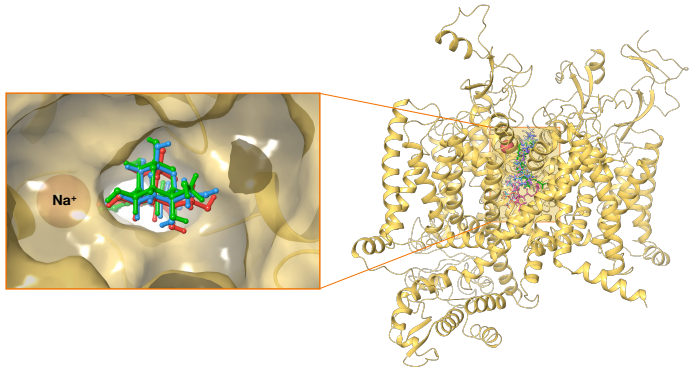

Fig. 5 Left panel: superposition of the structures of TTX in the core pore environment of Na_vPaS: crystallographic structure in blue and redocking geometry by Glide (red, RMSD = 0.62 Å) and METADOCK 2.0 (green, RMSD = 0.68 Å). Channel is displayed with yellow cartoons and surfaces. Na^+ is showed as a ball. Right panel: superposition of the predicted conformation for pyrethroids.

Glide (red) and METADOCK 2.0 (green). It can be shown that both predicted poses match the same location occupied by TTX in the core pore, which is associated to a root mean square deviation (RMSD) of 0.62 and 0.68 Å only for Glide and METADOCK 2.0 respectively. The benchmark step was completed by mimicking the conformation of six pyrethroids including Prallethrin, which was used as experimental control. As discussed, pyrethroids are reported as well-known inhibitors of American cockroach sodium channel.[52] The right-hand panel of Figure 5 shows illustrated that they are correctly docked into the central core of Na_vPaS by both Glide and METADOCK 2.0.

Finally, the binding energies for compounds used as a baseline (i.e., TTX and pyrethroids) are computed. These figures establish a binding energy threshold in order to figure out compounds that may exceed this threshold and thus could be considered as potential inhibitors of Na_vPaS. To homegeneize binding energy figures between Glide and METADOCK 2.0, we use the MMGBSA refinement. This process results in a binding energy of -47.74 kcal mol^{-1} (Glide) and -51.77 kcal mol^{-1} (METADOCK 2.0) for TTX respectively. Pyretrhorids reach the core pore with higher binding energies, showing Pyrethrin the highest affinity (-51.72 kcal mol^{-1}), followed by piperonyl butoxide (-48.13 kcal mol^{-1}). The other pyrethroids lies in the range of $-46/-35$ kcal mol^{-1}.

3.2 Computational screening

Even though the main goal is designing for an efficient strategy for the discover of novel insecticides, computational cost is a major parameter in any VS procedure. Consequently, this section reports the discovered compounds as well as the required resources for completing each of the proposed VS steps.

Glide VS-workflow is initiated with the HTVS step, which used the DB database as an input, i.e. 9137 compounds. All Glide parameters are set up as default. In that standard protocol, 10% of all compounds are retained for next steps, so that HTVS generates 913 candidate compounds as output. The overall execution time of the HTVS procedure was 51 minutes. The 913 selected compounds next fed into the SP procedure, which is completed in 1 hour and 11 minutes. SP generates 100 candidate compounds as output that were selected for the last stage of the VS pipeline. It is actually this last stage what makes different both workflows. In the Glide-based workflow, docking simulations of these 100 compounds with the active site of the Na_vPaS was assessed with the more refined XP regime, in which up to 10 conformations per compound are retrained. That final docking required 7 hour and 42 minutes of execution time on the CPU, meaning an average of ca. 277 seconds per compound. The standard VS-workflow is completed by computing the binding-free energy of the top-ranked compounds, which run for 1 hour and 24 minutes. For the records, Glide and MMGBSA simulations have been carried out in a 12-core 2.4GHz Intel Xeon™ workstation E5 2600v3, endowed with 23GB DDDR4 RAM Memory, 256-GB SSD Hard Disk.

As sketched in Figure 3, METADOCK 2.0 workflow also performed a simulation with the 100 previously selected compounds. However, contrary to Glide, METADOCK 2.0 goes for a blind (systematic) docking by assessing the interaction at all 1,377 alpha carbons (spots) throughout the sodium channel surface. It is worth stressing the initial population generated is 300 †. Next, a total of 413,100 different conformations were generated throughout the sodium channel surface, i.e., 1,377 alpha carbons $\times$ 300 individuals at each spot. A GPU-accelerated code is therefore a must to perform such blind-docking simulations in complex biosystems as Na_vPaS. Indeed, even with that large number of conformations, the METADOCK 2.0 is able to process these 100 compounds in 8 hours and 51 minutes only. That performance lead to an average execution time of 306 seconds per compounds when running in a NVIDIA A100 device with 6912 CUDA cores, 40 GB of HBM2 memory and 1.9 TB/seconds. The speed up of blind docking simulations becomes possible as METADOCK 2.0 was developed from scratch on CUDA programming language, so that is fully compatible with NVIDIA GPUs. Even if Glide and METADOCK 2.0 underling models rely on dissimilar theoretical background, it is worth noting that METADOCK 2.0 took only 0.74 milliseconds per pose, significantly faster than the 27.72 seconds per pose of Glide, more than four orders of magnitude of difference. We finally select best 100 conformations of each ligand (10,000 conformations) that undergo MMGBSA refinement, with a cost of 166 hours and 31 minutes.

We should note that numeric outputs by Glide and METADOCK 2.0 are not directly comparable as they rely on different scoring functions. As discussed, the use of MMGBSA allows us to refine the results, while homogenising the binding energies obtained by

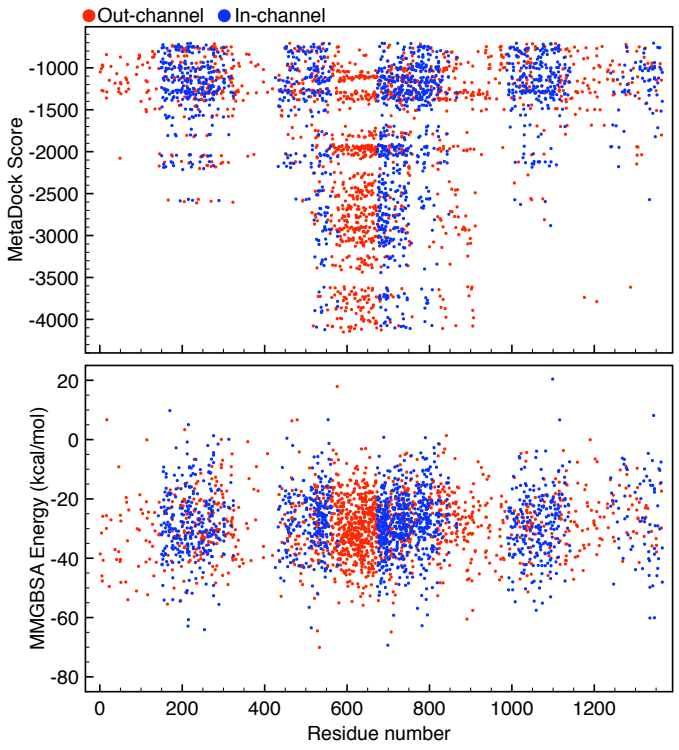

Fig. 6 Results with METADOCK 2.0 (top panel) and subsequent rescoring of all generated conformations with MMGBSA (bottom panel). As a blind docking, the whole surface of theNa_vPaS target is explored. Conformations inside of the core pore are displayed in blue (in channel) otherwise conformations are represented by red spots (out-channel).

both methods. An inspection of Figure 3 reveals one of the main differences between the standard workflow Glide–MMGBSA and the enhanced sampling with METADOCK 2.0–MMGBSA. The former approaches conducts VS at the binding site (core pore) while the latter explores the whole structure of the Na_vPaS target. As a consequence, all conformations predicted by Glide are located "in-channel". On the contrary, METADOCK 2.0 located conformations "in-channel" (in the core pore, as TTX and Na^+ cation) and "out-channel". Top panel of Figure 6 classifies METADOCK 2.0 conformations according to the computed score values *vs.* residue number of the selected spot (see Section "VS pipeline"). Conformations generated "in–channel" and "out–channel" are circled in blue and red, respectively.

It is worth noting the similar number of in– and out–conformations provided by METADOCK 2.0. This finding demonstrates that ligands might target several residues. It is also remarkable that METADOCK 2.0 predicts three residue areas: 0–400, 400–900 and 900–1300, approximately. The largest interaction (more negative METADOCK 2.0 score) lies in the region of residues 500–900. A visual inspection demonstrated that not all these residues correspond to the core pore. As a consequence, a site-guided VS might produce a limited picture of the binding mode to target Na_vPaS. Bottom panel represent the interaction energies of METADOCK conformations after MMGBSA refinement. Refinement by MMGBSA significantly impacts in the raking by METADOCK 2.0 by compacting the energetic dispersion. Indeed, three residue regions are still visible, though conformations with the largest binding energy "in-channel" (threshold of -60 kcal mol^{-1}) are now detected in these three residue areas. Compounds "in-channel" with the highest binding energies are extracted to complete our computational analysis.

Table 1 lists the best compounds obtained by the two proposed VS workflows. As demonstrated by numeric results, there is not a linear correlation between docking scores and MMGBSA interactions energies, conclusions that are valid for both Glide and METADOCK 2.0. As expected, docking is a valuable tool to assess possible binding modes (conformations) of drugs inside biomolecule pockets. However, interaction energies need to be further refinement with more advanced levels of theory. Such post-processing seems to be mandatory independently of the used docking engine. In addition, Table 1 demonstrates that conformations generated with METADOCK 2.0 are largely anchored to the Na_vPaS target. Standard Glide–MMGBSA workflow yields to a energetic window of $-57.86/-33.75$ kcal mol^{-1} in contrast with the more negative values derived from the METADOCK 2.0–MMGBSA sampling, with a top-ranked list with energies in the range of $-68.56/-51.88$ kcal mol^{-1}. These numeric outcomes hint that METADOCK 2.0 increases the interaction with the target by stabilizing the pose, a results that might be directly related with the larger amount of the generated conformations.

Regarding the chemical nature of the top-ranked compounds, standard workflow locates dihydrostreptomycin as the best-ranked MMGBSA hit ($\Delta G_{bind}^{MMGBSA} = -57.86$ kcal mol^{-1}), more negative than the energy computed for the crystallographic TTX in the Glide–MMGBSA framework ($\Delta G_{bind}^{MMGBSA} = -47.74$ kcal mol^{-1}). Dihydrostreptomycin is an aminoglycoside antibiotic

Table 1 Top-ranked compounds predicted by the standard Schröndinger protocol (Glide score, in kcal mol^{-1}) and by sampling with blind-docking METADOCK 2.0. The results shown here correspond to the MMGBSA output for a better comparison between methods. (ΔG_{bind}^{MMGBSA}, in kcal mol. Only molecules inside the channel are retained for discussion

Standard workflow		
Molecule[a]	Glide	ΔG_{bind}^{MMGBSA}
Dihydrostreptomycin	-7.01	-57.86
Bedoradrine	-4.31	-56.41
DB02732	-8.05	-55.97
DB01721	-3.80	-50.68
Plazomicin	-11.30	-49.59
Capivasertib	-0.32	-49.26
Netilmicin	-6.12	-44.34
Indinavir	-0.60	-42.75
Imidurea	-6.94	-40.86
Acarbose	-7.79	-34.91
Miglitol	-7.83	-33.75
Enhanced sampling		
Molecule[a]	METADOCK 2.0	ΔG_{bind}^{MMGBSA}
Nicofuranose	-957.84	-68.56
Milvexian	-757.69	-67.04
Aminoquinuride	-1371.98	-61.20
DB02498	-4094.25	-60.92
DB01690	-3706.87	-60.41
Acteoside	-1490.07	-60.30
DB02629	-1319.10	-59.77
Plazomicin	-2155.52	-58.85
Diquafosol	-3761.54	-53.81
Acarbose	-2139.54	-53.51
DB01763	-3657.78	-51.88

[a] Generic names are given when available

that. A contrasting picture is provided by our enhanced sampling scheme. As depicted in Table 1, METADOCK–MMGBSA locates nicofuranose, a niacin derivative used as a hypolipidemic agent, at the first place with a binding energy of $\Delta G_{bind}^{MMGBSA} = -68.56$ kcal mol^{-1}, which is the largest predicted interaction by our computational protocol. Until know, neither of these two molecules has been proposed as insecticide. Interestingly, the first placed molecules in these two lists do not appear in their counterpart. Diving into the lists (i.e., less negative MMGBSA values), the first match is reached with plazomicin that ranks fifth in the standard workflow ($\Delta G_{bind}^{MMGBSA} - 49.59$ kcal mol^{-1}) *vs.* eight at the enhanced sampling ($\Delta G_{bind}^{MMGBSA} - 58.85$ kcal mol^{-1}). A close inspection of Table 1 shows that plazomicin also exhibits a significant negative values in both Glide (-11.30 kcal mol^{-1}) and METADOCK 2.0 (-2155.52) scales. This compound (originally labelled as ACHN-490) is a next-generation aminoglycoside derivative with a potent clinical antibiotic activity.[53] It has been approved by the Food and Drug Administration (FDA) in 2018 for the treatment of infections caused by the multidrug-resistant *Enterobacteriaceae*.[54] It is remarkable that one of the associated side effects associated to aminoglycoside antibiotics is neuromuscular blockade. That undesirable effect is due to the interaction with channel proteins. Aminoglycosides might act as pore blockers at some voltage-dependent channels, including Ca^{2+} and K^+ channels.[55] As demonstrated by Wright and co-workers,[56] aminoglycosides are also able to inhibit sodium channels in *in vivo* rat models. That earlier evidence further support our discover, and consolidate plazomicin as a novel-promising Na_vPaS blocking. One might also note a second match, e.g., acarbose, which is associ-

ated to less negative binding energies though still present in both lists at tenth position.

Unfortunately, the top candidate in the enhanced sampling (nicofuranose) and in the consensus ranking (plazomicin) are either commercially unavailable or associated to prohibitive prices for developing industrial insecticide applications. Consequently, we decided to expand our search by moving down in the ranked list. As noted above, METADOCK–MMGBSA detected several compounds with larger binding energy "in-channel" (threshold of -60 kcal mol^{-1}). As for Glide–MMGBSA is concerned, more moderate values are observed. Consequently, we expand our search in the for the standard workflow by imposing the energetic window of pyrethroids (ca. $-48/-35$ kcal mol^{-1}, see Target Validation). All compounds that satisfied these inclusion criteria are listed in Table 1. A systematic search was conducted in commercial vendors to identity purchasable candidates, which passed to the final *in vivo* testing stage.

3.3 *In vivo* testing

Computational predictions were confirmed by assessing the biological of the commercially available candidates, e.g., miglitol, acarbose, netilmicin sulfate, capivasertib and dihydrostreptomycin. Prallethrin as a control pyrethroid (with purity higher than 98%). Table 2 shows test solutions (TS) for topical application on cockroaches. TS are divided into three groups: (1) solutions to evaluate the insecticidal capability of candidate molecules (TS$_x$I), which are composed of 3% of these molecules diluted in a suitable solvent; (2) solutions to evaluate the synergistic capability of candidate molecules (TS$_x$S) when applied in solution together with a pyrethroid; and (3) control solutions (TS$_x$C) which does not include candidate molecules in the solution to evaluate the starting point.

For the sake of validation, the solvent with the highest chemical affinity has been selected for each candidate molecule to achieve the desired concentration. These solvents were previously tested for toxicity by applying topically to the cockroaches a solution consisting of 100% of each solvent. All these tests were negative. Secondly, TS$_x$S-based solutions also include prallethrin at 0.05% concentration. This dose has been experimentally set as the minimum lethal dose in the target insect that allows us to evaluate the synergistic effect. Prallethrin is a pyrethroid widely used in commercial cockroach insecticides, as it is low cost and offers an optimal dose/response ratio. Finally, three control solutions (i.e., TS$_x$C) are also designed by combining solvents (DMF, DMSO and Water) and 0.05% prallethrin. In the case of the TS$_3$S solution, several emulsifiers have been used (TWEEN 20, EMULSOGEN TS100, CALSOGEN 4814, SABOWAX EL-H-40) that allow the netilmicin sulfate molecule to be solubilized in water. Table 2 also lists the received dose (in mg), which corresponds to an application of 5 μl per insect as noted in Section 3.3.

Our first attempt was conducted with drugs in absence of any other molecule (see TS$_x$I formulations in Table 2). Only miglitol leads to a positive but moderate result with 2 out of 6 cockroaches died after 24 hours (33% 24-hour mortality). In addition, none of them died during first 60 minutes. Such low-ratio

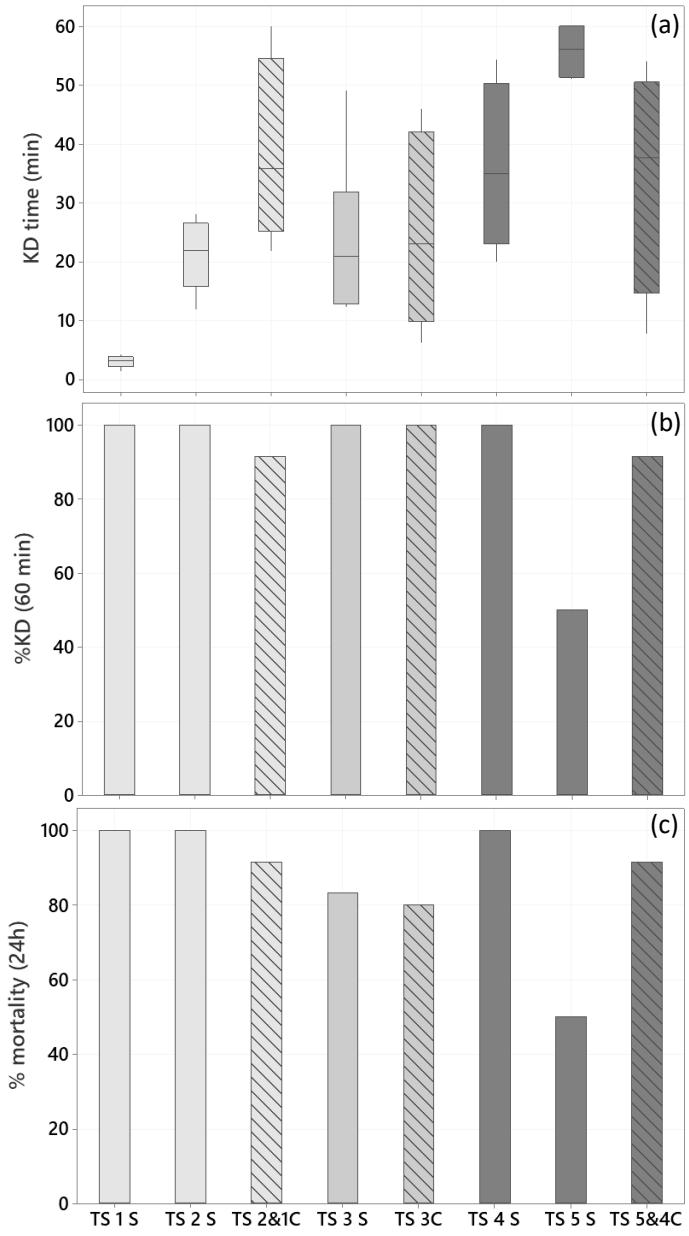

Fig. 7 *In vivo* outcomes after the use of the selected test solutions (ID). From top to bottom: (a) KD time in minutes (min) for the different mixtures under study; (b) percentage of the total cockroach population that have flipped over after 60 minutes; (c) Percentage of the total cockroach population that have been died after 24 hours.

of efficiency is not compatible with real commercial applications. Therefore, we can rule out the insecticidal effect of the isolated compounds, which motivates the evaluation of possible synergistic effects (TS$_x$S solutions listed in Table 2).

Figure 7 summarizes these *in vivo* metrics. Top panel (chart a) displays the KD time (in minutes) of these solutions. As shown, the miglitol-based solution (TS$_1$S) outperforms all other formulations. All cockroaches are flipped in less than five minutes. This is one of our most remarkable findings: miglitol speeds knockout up by a factor of 12X compared to controls. The second best-ranked solution corresponds to acarbose (TS$_2$S), with a KD

Table 2 Composition of test solutions designed to to assess insecticide efficiency (TS_xI), synergistic effects (TS_xS) and control (TS_xC) in cockroaches models

ID	Molecule	Molecule (%-mg)	Pyrethroid	Pyrethroid (%-mg)	Solvent	Solvent (%-mg)
TS_1I	Miglitol	3.00-0.143	–	–	DMF	97.00-4.626
TS_1S	Miglitol	3.00-0.143	Prallethrin	0.05-0.0024	DMF	96.95-4.626
TS_2I	Acarbose	3.00-0.144	–	–	DMF	97.00-4.639
TS_2S	Acarbose	3.00-0.144	Prallethrin	0.05-0.0024	DMF	96.95-4.639
					WATER	92.00-4.534
					TWEEN 20	1.80-0.090
TS_3I	Netilmicin sulfate	3.00-0.148	–	–	EMULSOGEN TS100	0.80-0.040
					CALSOGEN 4814	0.80-0.040
					SABOWAX EL-H-40	1.80-0.090
					WATER	91.95-4.534
					TWEEN 20	1.80-0.090
TS_3S	Netilmicin sulfate	3.00-0.148	Prallethrin	0.05-0.0025	EMULSOGEN TS100	0.80-0.040
					CALSOGEN 4814	0.80-0.040
					SABOWAX EL-H-40	1.80-0.090
TS_4I	Capivasertib	3.00-0.166	–	–	DMSO	97.00-5.367
TS_4S	Capivasertib	3.00-0.166	Prallethrin	0.05-0.0028	DMSO	96.95-5.367
TS_5I	Dihydrostreptomycin	3.00-0.167	–	–	DMSO	97.00-5.406
TS_5S	Dihydrostreptomycin	3.00-0.167	Prallethrin	0.05-0.0028	DMSO	96.95-5.406
$TS_{2\&1}C$	–	–	Prallethrin	0.05-0.0024	DMF	99.95-4.718
					WATER	94.95-4.761
					TWEEN 20	1.80-0.090
TS_3C	–	–	Prallethrin	0.05-0.0025	EMULSOGEN TS100	0.80-0.040
					CALSOGEN 4814	0.80-0.040
					SABOWAX EL-H-40	1.80-0.090
$TS_{5\&4}C$	–	–	Prallethrin	0.05-0.0028	DMSO	99.95-5.498

time of around 20 minutes. However, none o the other mixtures (TS_3S, TS_4S, TS_5S) leads to measurable synergistic effect when combined with prallethrin. Figure 7 also plots the percentage of the total population of cockroaches that have flipped over after 60 minutes (chart b) and the mortality after 24 hours (chart c) from the application. These metrics might differ as the insects may initially be affected due to the nerve impulses caused by the action of the test molecules, but a cockroach may recover shortly thereafter. Indeed, this outcome is reflected Figure 7 (charts b and c) where the percentage of mortality is reduced from 60 minutes to 24 hours in TS_3S and TS_3C solutions. That limitation is not observed neither in TS_1S nor TS_2S: the 100% of flip is retained at both 60 minutes and 24 hours. All accumulated results reveal the potential use of acarbose and, especially, miglitol as a synergistic for insecticides.

4 Conclusions

The present contribution deals with the use of molecular and experimental models to search for new inhibitor of voltage-gated sodium channel from the American cockroach *Periplaneta americana* (Na_vPaS). Our main goal is to enhance current insecticide formulations. A systematic virtual screening (VS) of the Drug Bank (DB) database is presented through two levels of theory (Glide and METADOCK 2.0). The resulting list of compounds was further refined with MMGBSA rescoring to generate a ranked list of chemical based on to their ability to reach and block the core pore.

There is one critical parameter that was not directly included in our molecular models: commercial availability. If real industrial applications are sought, the proposed insecticide must be accessible at a low cost. Among all selected hits, 5 compounds were purchasable. Miglitol, acarbose, netilmicin sulfate, capivasertib and dihydrostreptomycin are available at a cost of less $400 USD per 5 g, significantly cheaper than the reference prallethrin, which is available with a cost of ca. $2000 USD per 5g. All were tested *in vivo* with cockroach models and compared to current prallethrin-based household insecticides. Our experimental results hint that miglitol is a potent synergistic for killing the American cockroach. The performed *in vivo* assays demonstrated that miglitol accelerates the knockdown by 12 times while simultaneously offering 100% mortality rate. Arcabose (one of the candidates that appears in both computational schemes) has also shown very promising results, reducing the knockdown time by 2X factor and also showing 100% mortality rate.

Of course, we do not claim to have performed here a complete search of all other targets in the insecticide activity observed for miglitol and acarbose. Indeed, both molecules are α-glucosidase inhibitors used for antidiabetic drugs.[57] Consequently, more extended computational and *in vivo* assays must be performed by including additional model systems and/or other pyrethroid combinations. The present contribution is a first step towards the discover of that new generation of broad-spectrum synergists.

List of abbreviations

VS: virtual screening; DB: drug bank; WHO: World Health Organisation; Na_v: voltage-activated sodium channels; Na_vPaS:

voltage-activated sodium channels from American cockroach; VGSC: voltage-dependent sodium channel; KD: knockdown time; PDB: protein data bank; TTX: tetrodotoxin; HTVS: high throughput virtual screening; SP: standard precision; XP: extra precision; CPU: central processing unit; GPU: graphics processing unit; GA: genetic algorithm; GS: greedy search algorithm; SS: scatter search algorithm; MMGBSA: molecular mechanics/generalized Born surface area method; SASA: solvent-accessible surface area; CUDA: Compute Unified Device Architecture; FDA: Food and Drug Administration; TS: test solutions; DMF: dimethylformamide, DMSO: dimethylsulfoxide.

Conflicts of interest

The authors are inventors of a patent application for use of miglitol as a synergistic compound in insecticide formulations (P202230916).

Acknowledgements

This work has been funded by the Ramón y Cajal Grant num. RYC2018-025580-I, funded by MCIN/AEI/10.13039/501100011033 and by FSE invest in your future. Bio Logic Crop Science, S.L. and UCAM industrial doctorate program have also participated in the financing of this work. The author is grateful for the computing resources (the Picasso supercomputer), technical expertise and assistance provided by the SCBI (Supercomputing and Bioinformatics) center of the University of Malaga, a member of the Plataforma Andaluza de Bioniformática.

Notes and references

1 Y. Chen, M. He, Z.-Q. Li, Y.-N. Zhang and P. He, *Scientific reports*, 2016, **6**, 1–12.

2 J. Zhang, Y. Zhang, J. Li, M. Liu and Z. Liu, *PloS one*, 2016, **11**, e0155254.

3 J. E. Jeong, H. J. Hwang, H. S. Park, H. J. Cha, Y. S. Lee and M. Ock, *Genes & Genomics*, 2015, **37**, 271–280.

4 H. Nasirian, *Acta tropica*, 2017, **167**, 86–98.

5 X. Bonnefoy, H. Kampen and K. Sweeney, *Public health significance of urban pests*, World Health Organization, 2008.

6 G. J. Kaczorowski, O. B. McManus, B. T. Priest and M. L. Garcia, *The Journal of general physiology*, 2008, **131**, 399–405.

7 H. Shen, Q. Zhou, X. Pan, Z. Li, J. Wu and N. Yan, *Science*, 2017, **355**, year.

8 L. M. Field, T. E. Davies, A. O. O'reilly, M. S. Williamson and B. A. Wallace, *European Biophysics Journal*, 2017, **46**, 675–679.

9 T. Davies, L. Field, P. Usherwood and M. Williamson, *IUBMB life*, 2007, **59**, 151–162.

10 J. Gan, S. Lee, W. Liu, D. Haver and J. Kabashima, *Journal of Environmental Quality*, 2005, **34**, 836–841.

11 S. Ullah, Z. Li, A. Zuberi, M. Z. U. Arifeen and M. M. F. A. Baig, *Environmental Chemistry Letters*, 2019, **17**, 945–973.

12 M. Ahmed and F. Matsumura, *Journal of medical entomology*, 2014, **49**, 1405–1410.

13 J. Drews, *Science*, 2000, **287**, 1960–1964.

14 U. Rester, *Current opinion in drug discovery & development*, 2008, **11**, 559–568.

15 J. M. R. et al., *Natural Compounds as Drugs Volume I*, Springer, 2008, pp. 211–249.

16 N. S. Pagadala, K. Syed and J. Tuszynski, *Biophysical reviews*, 2017, **9**, 91–102.

17 G. M. Morris, D. S. Goodsell, R. S. Halliday, R. Huey, W. E. Hart, R. K. Belew and A. J. Olson, *Journal of Computational Chemistry*, 1998, **19**, 1639–1662.

18 R. F. et al., *Journal of Medicinal Chemistry*, 2004, **47**, 1739–1749.

19 S. McIntosh-Smith, J. Price, R. B. Sessions and A. A. Ibarra, *The international journal of high performance computing applications*, 2015, **29**, 119–134.

20 T. J. Ewing, S. Makino, A. G. Skillman and I. D. Kuntz, *Journal of computer-aided molecular design*, 2001, **15**, 411–428.

21 I. Sánchez-Linares, H. Pérez-Sánchez, J. M. Cecilia and J. M. García, *BMC bioinformatics*, 2012, **13**, 1–14.

22 B. Imbernón, J. M. Cecilia, Horacio and D. Giménez, *The International Journal of High Performance Computing Applications*, 2017, 1–15.

23 B. Imbernón, A. Serrano, A. Bueno-Crespo, J. L. Abellán, H. Pérez-Sánchez and J. M. Cecilia, *Bioinformatics*, 2021, **37**, 1515–1520.

24 G. Schneider, *Drug Discovery Today*, 2002, **7**, 64–70.

25 A. N. Jain, *Current Protein and Peptide Science*, 2006, **7**, 407–420.

26 J. Lacroix, F. Campos, L. Frezza and F. Bezanilla, *Nueron*, 2013, **79**, 651–657.

27 K. Dong, *Invert Neurosci.*, 2007, **7**, 17–30.

28 H. Shen, Z. Li, Y. Jiang, X. Pan, J. Wu, B. Cristofori-Armstrong, J. J. Smith, Y. K. Chin, J. Lei, Q. Zhou *et al.*, *Science*, 2018, **362**, year.

29 *Schrödinger Release 2023-1*, 2023, Epik Schrödinger, LLC, New York, 2021.

30 G. Madhavi Sastry, M. Adzhigirey, T. Day, R. Annabhimoju and W. Sherman, *J. Comput. Aided Mol. Des.*, 2013, **27**, 221–234.

31 J. C. Shelley, A. Cholleti, L. L. Frye, J. R. Greenwood, M. R. Timlin and M. Uchimaya, *J. Comput. Aided Mol. Des.*, 2007, **21**, 681–691.

32 M. H. M. Olsson, C. R. Søndergaard, M. Rostkowski and J. H. Jensen, *J. Chem. Theory Comput.*, 2011, **7**, 525–537.

33 C. Lu, C. Wu, D. Ghoreishi, W. Chen, L. Wang, W. Damm, G. A. Ross, M. K. Dahlgren, E. Russell, C. D. Von Bargen, R. Abel, R. A. Friesner and E. D. Harder, *J. Chem. Theory Comput.*, 2021, **17**, 4291–4300.

34 D. S. Wishart, C. Knox, A. C. Guo, D. Cheng, S. Shrivastava, D. Tzur, B. Gautam and M. Hassanali, *Nucleic acids research*, 2008, **36**, D901–D906.

35 J. Wang, *J. Chem. Inf. Model.*, 2020, **60**, 1549–9596.

36 *Schrödinger Release 2023-1: LigPrep*, 2023, Schrödinger, LLC, New York, NY.

37 T. A. Halgren, R. B. Murphy, R. A. Friesner, H. S. Beard, L. L.

Frye, W. T. Pollard and J. L. Banks, *Journal of Medicinal Chemistry*, 2004, **47**, 1750–1759.
38 R. A. Friesner, J. L. Banks, R. B. Murphy, T. A. Halgren, J. J. Klicic, D. T. Mainz, M. P. Repasky, E. H. Knoll, M. Shelley, J. K. Perry, D. E. Shaw, P. Francis and P. S. Shenkin, *Journal of Medicinal Chemistry*, 2004, **47**, 1739–1749.
39 R. A. Friesner, R. B. Murphy, M. P. Repasky, L. L. Frye, J. R. Greenwood, T. A. Halgren, P. C. Sanschagrin and D. T. Mainz, *Journal of Medicinal Chemistry*, 2006, **49**, 6177–6196.
40 B. Imbernón, J. M. Cecilia, J.-M. Cutillas-Lozano and D. Giménez, Proceedings of the 47th International Conference on Parallel Processing Companion, 2018, pp. 1–8.
41 B. Imbernón, A. Llanes, J.-M. Cutillas-Lozano and D. Giménez, *The International Journal of High Performance Computing Applications*, 2020, **34**, 30–41.
42 O. Trott and A. J. Olson, *Journal of computational chemistry*, 2010, **31**, 455–461.
43 G. M. Morris, R. Huey, W. Lindstrom, M. F. Sanner, R. K. Belew, D. S. Goodsell and A. J. Olson, *Journal of computational chemistry*, 2009, **30**, 2785–2791.
44 J. P. Cerón-Carrasco, *ChemMedChem*, 2022, **17**, e202200278.
45 M. P. Jacobson, R. A. Friesner, Z. Xiang and B. Honig, *Journal of Molecular Biology*, 2002, **320**, 597–608.
46 M. P. Jacobson, D. L. Pincus, C. S. Rapp, T. J. Day, B. Honig, D. E. Shaw and R. A. Friesner, *Proteins: Structure, Function, and Bioinformatics*, 2004, **55**, 351–367.
47 T. Hou, J. Wang, Y. Li and W. Wang, *Journal of Chemical Information and Modeling*, 2011, **51**, 69–82.
48 G. Rastelli, A. D. Rio, G. Degliesposti and M. Sgobba, *Journal of Computational Chemistry*, 2010, **31**, 797–810.
49 S. P. Niinivehmas, S. I. Virtanen, J. V. Lehtonen, P. A. Postila and O. T. Pentikäinen, *Journal of Chemical Information and Modeling*, 2011, **51**, 1353–1363.
50 M. Ylilauri and O. T. Pentikäinen, *Journal of Chemical Information and Modeling*, 2013, **53**, 2626–2633.
51 P.-C. Su, C.-C. Tsai, S. Mehboob, K. E. Hevener and M. E. Johnson, *Journal of Computational Chemistry*, 2015, **36**, 1859–1873.
52 D. M. Soderlund, *Archives of toxicology*, 2012, **86**, 165–181.
53 E. S. Armstrong and G. H. Miller, *Current Opinion in Microbiology*, 2010, **13**, 565–573.
54 G. Cox, L. Ejim, P. J. Stogios, K. Koteva, E. Bordeleau, E. Evdokimova, A. O. Sieron, A. Savchenko, A. W. Serio, K. M. Krause and G. D. Wright, *ACS Infectious Diseases*, 2018, **4**, 980–987.
55 K. Nomura, K. Naruse, K. Watanabe and M. Sokabe, *J Membr Biol*, 1990, **115**, 241–251.
56 A. J. Yeiser, J. R. Cox and S. N. Wright, *Pflügers Archiv*, 2004, **448**, 204–213.
57 P. H. Joubert, H. L. Venter and G. N. Foukaridis, *Br. J. Clin. Pharmacol.*, 1990, **30**, 391–396.

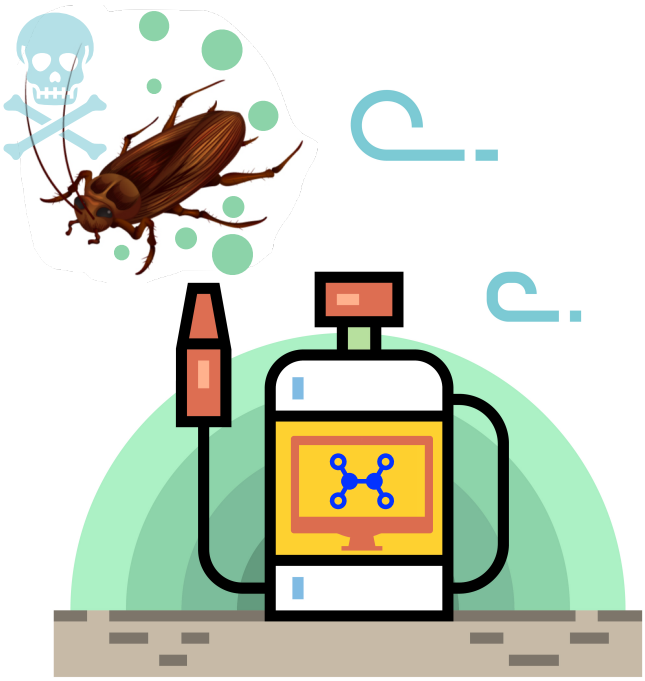

Table of contents

SUPPORTING INFORMATION TO

Insecticide discovery by drug repurposing: new synergistic inhibitors against Periplaneta americana

Beatriz Chafer-Dolz,*,† José M. Cecilia,‡ Baldomero Imbernón,¶ Estrella Núñez-Delicado,¶ Victor Casaa-Giner,† and José P. Cerón-Carrasco*,§

†*Bio Logic Crop Science, S.L. Amadeo de Saboya 1-4, 46010, Valencia, Spain*

‡*Universitat Politcnica de Valncia (UPV). Camino de Vera S/N, 46022, Valencia, Spain.*

¶*Universidad Católica San Antonio de Murcia (UCAM). Campus de los Jerónimos, 30107, Murcia, Spain.*

§*Centro Universitario de la Defensa. Universidad Politécnica de Cartagena. Base Aerea de San Javier, C/ Coronel López Peña s/n 30729. Santiago de la Ribera, Murcia, Spain.*

E-mail: bchafer@biologiccropscience.com; jose.ceron@cud.upct.es

Workflow overview

In our contribution, we propose a Virtual Screening (VS) pipeline to find new chemical compounds that inhibit the American cockroach Na_vPaS, and may eventually act as synergistic of current insecticides to improve their response and/or mortality, by screening the Drug Bank (DB) database that contains ca 10000 compounds.

Our VS methodology uses two ligand-based VS procedures; the commercial Glide solution, one of the industry standard in VS investigations, and the recently developed METADOCK 2.0, which provides a blind docking search by scanning the whole target surface. These energy interactions, obtained by Glide and METADOCK 2.0, are further refined by using MMGBSA rescoring to provide homogeneous energy interaction figures. Best ranked compounds are proposed for *in vivo* testing. This last step is determined by the availability of the identified products and/or their economic viability. The main contributions of the paper includes the following:

1. An in-depth VS procedure is proposed, combining two different ligand-based docking approaches and curating their results by MMGBSA rescoring. METADOCK 2.0 has higher throughput in terms of the number of conformations simulated; 0.74 miliseconds/pose (METADOCK 2.0) *vs.* 27.72 seconds/pose (Glide). Moreover, METADOCK 2.0 increases the interaction with the target by stabilizing the pose, offering wider picture of the binding mode to target Na_vPaS.

2. The DB database is fully screened virtually for Na_vPaS inhibitors of the American cockroach. Best-ranked compounds are listed with high energy interaction figures.

3. A positive control is established with the predominant compound in household insecticides to eliminate cockroaches (i.e. pyrethroids) to determine the energetic interaction threshold of the docking methods and also to validate our target (i.e. Na_vPaS).

4. Five compounds are tested with *in vivo* models, which lead to two novel synergistic compounds that improve the activity of currently used insecticides.

5. Our *in vivo* experimental results show that miglitol reduces the knockdown time by a factor of up to 12 times, from 60 minutes to 5 minutes, showing 100% of mortality rate.

METADOCK 2.0 is freely available on

`https://Baldoimbernon@bitbucket.org/Baldoimbernon/metadock_2.git.`

Computational Details

Table 1: The nineteen metaheuristic parameters used for $METADOCK2.0$.

Metaheuristic Parameters		Description
6*$ParamIni$	$INEIni$	Number of initial ligand conformations.
	$IIEFlex$	The intensification of the flexibility in the improvement functions.
	$PEIIni$	Percentage of the best conformations that are improved in the function Initialize.
	$IIEIni$	The intensification of the improvement in the function Initialize.
	$PBEIni$	Percentage of best conformations to be included in the initial set for the next iterations.\end{tabular
	$PWEIni$	Percentage of worst conformations to be included in the initial set for the next iterations.
2*$ParamSel$	$PBESel$	Percentage of the best conformations to be selected for combination.
	$PWESel$	Percentage of the worst conformations to be selected for combination.
3*$ParamCom$	$PBBCom$	Percentage of best-best conformations to be combined.
	$PWWCom$	Percentage of worst-worst conformations to be combined.
	$PBWCom$	Percentage of best-worst conformations to be combined.
2*$ParamMut$	$PMUCom$	Percentage of best conformations of the combination to be muted.
	$IMUCom$	The intensification of the mutation of elements generated by combination.
2*$ParamImp$	$PEIImp$	Percentage of best conformations of the combination to be improved.
	$IIEImp$	The intensification of the improvement of elements generated by combination.
$ParamInc$	$PBEInc$	Percentage of best conformations to be included in the reference set.
2*$ParamEnd$	$NIREnd$	Maximum number of steps without improvement.
	$MNIEnd$	Maximum number of iterations with or without improvement.

Table 2: Parameter setting selected by HYPERDOCK with which the METADOCK experiments have been developed.

INEIni	300	Number of initial ligand conformations.
IIEFlex	20	The intensification of the flexibility in the improvement functions.
PEIIni	100	Percentage of the best conformations that are improved in the function Initialize.
IIEIni	200	The intensification of the improvement in the function Initialize.
PBEIni	100	Percentage of best conformations to be included in the initial set for the next iterations.
PWEIni	0	Percentage of worst conformations to be included in the initial set for the next iterations.
PBESel	50	Percentage of the best conformations to be selected for combination.
PWESel	50	Percentage of the worst conformations to be selected for combination.
PBBCom	50	Percentage of best-best conformations to be combined.
PWWCom	20	Percentage of worst-worst conformations to be combined.
PBWCom	10	Percentage of best-worst conformations to be combined.
PMUCom	20	Percentage of best conformations of the combination to be muted.
IMUCom	10	The intensification of the mutation of elements generated by combination.
PEIImp	50	Percentage of best conformations of the combination to be improved.
IIEImp	100	The intensification of the improvement of elements generated by combination.
PBEInc	50	Percentage of best conformations to be included in the reference set.
NIREnd	3	Maximum number of steps without improvement.
MNIEnd	3	Maximum number of iterations with or without improvement.

Table 3: Main active ingredients, solvents and emulsifiers used for *in vivo* testing

CAS number	Materials	Supplier
72432-03-2	Miglitol	Target Molecule Corp.
56180-94-0	Acarbose	Glentham Life Sciences Ltd
56391-57-2	Netilmicin sulfate	Glentham Life Sciences Ltd
1143532-39-1	Capivasertib	Target Molecule Corp.
128-46-1	Dihydrostreptomycin	Carbosynth Ltd
23031-36-9	Prallethrin	Endura S.p.A.
7732-18-5	Water	–
68-12-2	Dimethylformamide (DMF)	Fluorochem
67-68-5	Dimethyl sulfoxide (DMSO)	TCI EUROPE N.V
–	Tween 20	Croda Iberica SA
70559-25-0	Emulsogen TS100	Clariant Produkte (Deutschland) GmbH
–	Calsogen 4814	Clariant Produkte (Deutschland) GmbH
61788-85-0	Sabowax EL-H 40	SABO SpA